# Possible triplet $p + ip$ superconductivity in graphene at low filling

Tianxing Ma,[1,2] Fan Yang,[3,2,*] Hong Yao,[4,5,†] and Hai-Qing Lin[2]
[1]*Department of Physics, Beijing Normal University, Beijing 100875, China*
[2]*Beijing Computational Science Research Center, Beijing 100084, China*
[3]*School of Physics, Beijing Institute of Technology, Beijing 100081, China*
[4]*Institute of Advanced Study, Tsinghua University, Beijing 100084, China*
[5]*Collaborative Innovation Center of Quantum Matter, Beijing 100084, China*
(Received 19 March 2014; revised manuscript received 15 November 2014; published 4 December 2014)

We study the Hubbard model on the honeycomb lattice with nearest-neighbor hopping ($t > 0$) and next-nearest-neighbor hopping ($t' < 0$). When $t' < -t/6$, the single-particle spectrum is featured by the continuously distributed Van Hove saddle points at the band bottom, where the density of states diverges in a power law. We investigate possible unconventional superconductivity in such systems with the Fermi level close to the band bottom by employing both random-phase-approximation and determinant quantum Monte Carlo approaches. Our study reveals a possible triplet $p + ip$ superconductivity in this system with appropriate interactions. Our results might provide a possible route to look for triplet superconductivity with relatively high transition temperature in low-filled graphene and other similar systems.

DOI: 10.1103/PhysRevB.90.245114 PACS number(s): 72.80.Vp, 74.20.Mn, 74.20.Rp

## I. INTRODUCTION

Graphene, a single layer of carbon atoms forming a honeycomb lattice, has been among the most exciting research fields since it was synthesized [1]. For this remarkable material, enormous attention has been focused on exploring the physics related to its Dirac-cone band structure [2]. For graphene close to half filling, the density of states (DOS) at the Fermi level almost vanishes; as a consequence, relatively weak or intermediate short-range repulsive interactions in general do not induce phase transitions at low temperature [2]. Nonetheless, exotic phases might be induced by repulsive interactions when the Fermi level is a finite energy away from the Dirac point. For instance, it was shown by renormalization group (RG) calculations that unconventional or topological superconductivity (SC) is induced by weak repulsive interactions in honeycomb Hubbard models finitely away from half filling [3,4]. More recently, exotic phases such as $d + id$ [3,5–11] topological superconductivity [12,13] and Chern-band insulators with spin density waves [14,15] near the type-I Van Hove singularity (VHS) at $\frac{1}{4}$ electron or hole doping, where the DOS at the Fermi level diverges logarithmically. Such a logarithmically diverging DOS close a VHS may significantly raise the superconducting transition temperature. More recently, it was shown by RG analysis that topological triplet $p + ip$ superconductivity can generically occur in systems at a type-II VHS where the saddle points are not at a point of time-reversal-invariant momenta [16,17].

In two dimensions (2D), for a Fermi surface with discrete Van Hove saddle points, the DOS at the Fermi level diverges only logarithmically. It would be interesting to study phases in systems with a power-law diverging DOS. Indeed, it was shown that, for the hopping parameters satisfying $t' < -t/6$, an inverse-square-root diverging DOS occurs close to band bottom of the lower band, where the band bottom is a closed line instead of discrete points as shown in Fig. 1(b). In graphene, such hopping parameters are possible [18–20], and high levels of doping are have recently become experimentally accessible [21]. Note that the band bottom occurs at a closed line only when no third-neighbor or longer-range hopping is considered. This kind of line band bottom may be considered as a set of continuously distributed Van Hove (VH) saddle points. Recent determinant quantum Monte Carlo (DQMC) study has revealed ferromagnetic-like spin correlations in such systems [22], which implies the possibility of a dominant triplet pairing state in this system with repulsive interactions.

In this paper, we report both the random-phase-approximation (RPA) analysis and DQMC studies of pairing symmetries of possible SC induced by weak or intermediate repulsive interactions in graphene at low fillings whose DOS at the Fermi level is significantly enhanced by the power-law singularity at the band bottom. Both numerical approaches obtain the $p + ip$ triplet pairing as the leading instability of the system in different parameter regimes. For $t' = -0.2t$, $U/t = 3.0$, and filling $n = 0.2$, the transition temperature $T_{c,\text{triplet}}$ into the triplet pairing state is estimated to be on the order of $10^{-2}t$. For graphene, $t \sim 2.0$ eV, which implies that the $T_{c,\text{triplet}}$ in graphene might be as high as 200 K when the Fermi level is tuned appropriately close to the band bottom. These results might provide a possible route to look for triplet superconductivity with relatively high transition temperature in graphene at low filling.

## II. MODEL AND APPROACH

We start from the following Hubbard model on the honeycomb lattice:

$$H = -t \sum_{\langle i,j \rangle} c^\dagger_{i\sigma} c_{j\sigma} - t' \sum_{\langle\langle i,j \rangle\rangle} c^\dagger_{i\sigma} c_{j\sigma} + U \sum_i n_{i\uparrow} n_{i\downarrow}, \quad (1)$$

where $c^\dagger_{i\sigma}$ is the electron creation operator at site $i$ and with spin polarization $\sigma = \uparrow, \downarrow$ and $U$ labels the on-site repulsive interaction. Here the $t$ and $t'$ terms describe the nearest-

*yangfan_blg@bit.edu.cn
†yaohong@tsinghua.edu.cn

 

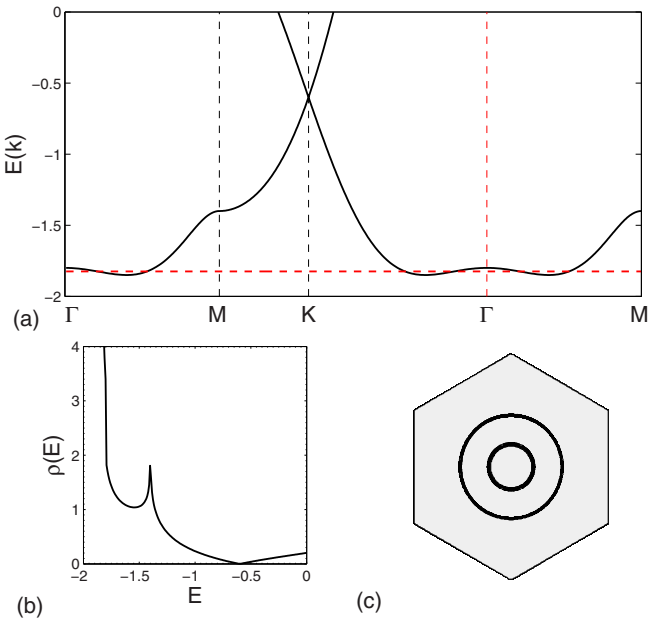


FIG. 1. (Color online) (a) The energy band along the high-symmetry line in the first Brillouin zone. (b) The DOS as a function of energy with $t' = -0.2t$. (c) The Fermi surface at filling $n = 0.2$.

neighbor (NN) and next-nearest-neighbor (NNN) hoppings, respectively. We consider the case of $t > 0$ and $t' < 0$, which is supported by recent first principle calculations [18] and experiments [19]. As the ratio $|\frac{t'}{t}|$ varies from around 0.1 [19] to around 0.3 [20] in different experiments, we focus on the possible cases with $t' < -t/6$ and take $t' = -0.2t$ in our calculations unless stated otherwise.

The band structure is shown in Fig. 1(a), together with the Fermi levels for filling $n = 0.2$ per site. We notice one remarkable feature of this band structure: the band bottom of this system is not located at the Γ point; instead it consists of two closed lines around Γ. As a consequence, the DOS is divergent in an inverse-square-root fashion near the band bottom, as shown in Fig. 1(b). The Fermi surface (FS) of the system at $n = 0.2$ is shown in Fig. 1(c), which contains an inner hole pocket and an outer electron pocket. Such a Hubbard model with only an on-site interaction has been widely used [5–7,9,10] to describe graphene doped to near the VH points because, at such dopings, the divergent DOS on the FS leads to strong screening of the Coulomb interaction.

In the following, we adopt perturbative RPA analysis for weak-$U$ interactions and the DQMC calculations for relatively strong $U$ to investigate the pairing symmetries of the possible SC at low filling.

## III. RANDOM-PHASE-APPROXIMATION TREATMENT

We adopted the standard multi-orbital RPA approach [23–28] in our study for the small-$U$ ($=0.1t$) case.

Various susceptibilities of noninteracting electrons of this system are defined as

$$\chi^{(0)l_1,l_2}_{l_3,l_4}(\mathbf{q},\tau) \equiv \frac{1}{N}\sum_{\mathbf{k_1},\mathbf{k_2}} \left\langle T_\tau c^\dagger_{l_1}(\mathbf{k_1},\tau) c_{l_2} \times (\mathbf{k_1}+\mathbf{q},\tau) c^+_{l_3}(\mathbf{k_2}+\mathbf{q},0) c_{l_4}(\mathbf{k_2},0)\right\rangle_0, \quad (2)$$

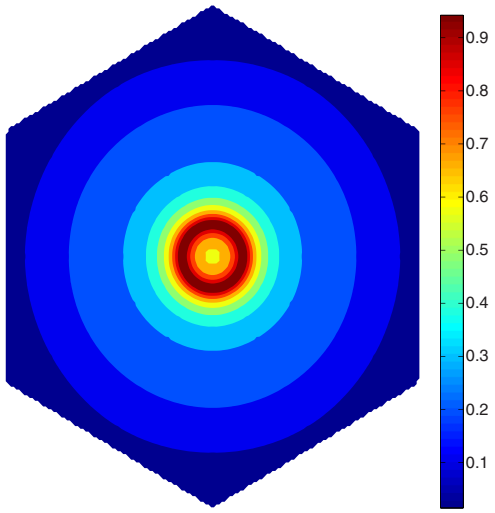


FIG. 2. (Color online) Largest eigenvalues of the susceptibility matrix in noninteracting limit in the first Brillouin zone.

where $l_i$ ($i = 1,2$) denotes the orbital (sublattice) index. The largest eigenvalues of the susceptibility matrix $\chi^{(0)}_{l,m}(\mathbf{q}) \equiv \chi^{(0)l,l}_{m,m}(\mathbf{q}, i\nu = 0)$ are shown in Fig. 2 for filling $n = 0.1$, which shows dominant distributions on a small circle around the Γ point. This suggests strong ferromagnetic-like intrasublattice spin fluctuations in the system. Generally, it is found that, at low fillings, the radius of the circle scales with filling. At low fillings, the eigenvector of the susceptibility matrix reveals that the intersublattice spin fluctuations in the system are also ferromagnetic like, although somewhat weaker than the intra-sublattice ones. Such ferromagnetic-like spin fluctuations are consistent with the ferromagnetic spin correlations revealed by the DQMC calculations [22].

With weak Hubbard $U$, the spin $\chi^s$ or charge $\chi^c$ susceptibilities in the RPA level are given by

$$\chi^{s(c)}(\mathbf{q}, i\nu) = [I \mp \chi^{(0)}(\mathbf{q}, i\nu)\bar{U}]^{-1}\chi^{(0)}(\mathbf{q}, i\nu), \quad (3)$$

where $\bar{U}^{\mu\nu}_{\mu'\nu'}$ ($\mu\nu = 1,2$) is a $4\times 4$ matrix whose only two nonzero elements are $\bar{U}^{11}_{11} = \bar{U}^{22}_{22} = U$. Clearly, the repulsive Hubbard $U$ suppresses $\chi^c$ but enhances $\chi^s$. Thus, the spin fluctuations take the main role of mediating the Cooper pairing in the interacting system [23]. At the RPA level, the Cooper pairs near the FS acquire an effective interaction $V_{\text{eff}}$ [23,24,28] by exchanging the spin fluctuations represented by the spin susceptibilities. From this effective interaction, one obtains the linearized gap equation near the superconducting critical temperature $T_c$, solving which gives the leading pairing symmetry (symmetries) of the system.

Our results for $n = 0.1$ and $n = 0.2$ reveal that the leading pairing symmetries of the system at these low fillings are degenerate $p_x$ and $p_y$ doublets, as shown in Figs. 3(a) and 3(b), which should be further mixed as $p_x \pm ip_y$ to minimize the ground-state energy, as suggested by our further mean-field calculations on the effective Hamiltonian. Such a triplet pairing is mediated by the ferromagnetic-like spin fluctuations in the system, as shown in Fig. 2. The subleading pairing symmetries of the system at these low fillings are triplet $f$ waves, as shown in Fig. 4(a) for $n = 0.1$, and singlet $d_{xy}$ and $d_{x^2-y^2}$ doublets

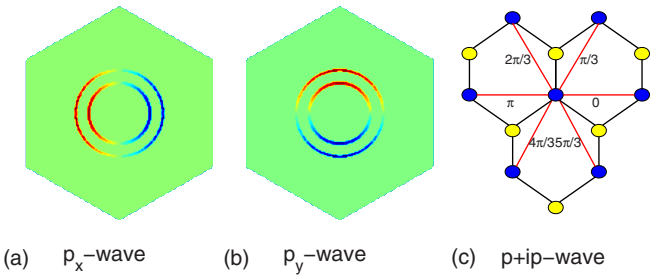


FIG. 3. (Color online) Panels (a) and (b) show the $p_x$ and $p_y$ pairing symmetries in $k$ space and panel (c) shows the phase of the $p+ip$ pairing symmetry on the honeycomb lattice in real space.

(which should further be mixed as $d_{xy} \pm id_{x^2-y^2}$ to lower the energy), as shown in Figs. 5(a) and 5(b) for $n = 0.2$.

Note that we have chosen $U$ as small as $U = 0.1t$ in our RPA calculations. For larger $U$ beyond its critical value $U_c$, the divergence of the spin susceptibility invalidates our RPA calculations for superconductivity. Physically, such a divergent spin susceptibility for $U > U_c$ may not necessarily lead to a magnetically ordered state since the distribution of the susceptibility shown in Fig. 2 does not possess a sharply peaked structure at a particular momentum. Instead, the competition among different wave vectors may lead to paramagnetic behavior or short-ranged spin correlations which provide a basis for the Cooper pairing. We leave the study for the case of $U > U_c$ to the following DQMC approach, which is suitable for strong-coupling problems.

## IV. DETERMINANT QUANTUM MONTE CARLO SIMULATIONS

The DQMC simulation is a powerful unbiased numerical tool to study the physical properties of strongly correlated electronic systems such as the Hubbard model. The basic strategy of DQMC is to express the partition function as a high-dimensional integral over a set of random auxiliary fields. The integral is then accomplished by Monte Carlo techniques. For more details on the technique, see Refs. [22,29,30].

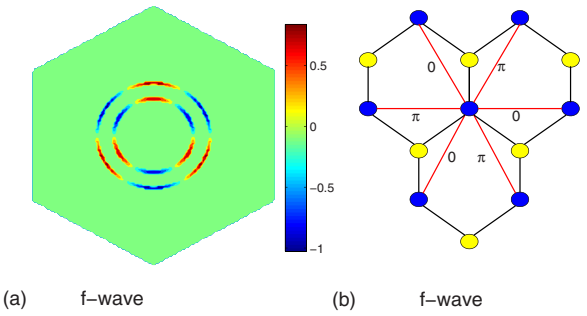


FIG. 4. (Color online) Panel (a) shows the $f$ pairing in $k$ space and panel (b) shows the phase of the $f$ pairing symmetries in real space.

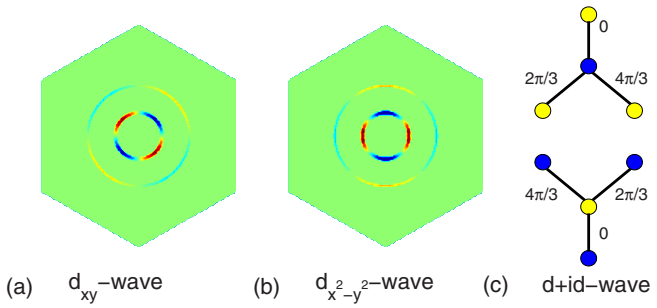


FIG. 5. (Color online) Panels (a) and (b) show the $d_{xy}$ and $d_{x^2-y^2}$ pairing symmetries in $k$ space and panel (c) shows the phase of the $d+id$ pairing symmetries in real space.

To investigate the SC property, we compute the pairing susceptibility

$$P_\alpha \equiv \frac{1}{N_s}\sum_{i,j}\int_0^\beta d\tau \langle \Delta_\alpha^\dagger(i,\tau)\Delta_\alpha(j,0)\rangle. \quad (4)$$

Here, $\alpha$ stands for the pairing symmetry, and the corresponding pairing order parameter $\Delta_\alpha^\dagger(i)$ is defined as

$$\Delta_\alpha^\dagger(i) \equiv \sum_l f_\alpha^*(\delta_l)(c_{i\uparrow}c_{i+\delta_l\downarrow} \pm c_{i\downarrow}c_{i+\delta_l\uparrow})^\dagger, \quad (5)$$

where $f_\alpha(\delta_l)$ is the form factor of the pairing function, the vectors $\delta_l$ denote the bond connections, and "−" ("+") labels singlet (triplet) symmetry.

Guided by the RPA results, three different pairing symmetries were investigated in the following DQMC studies, i.e., $p+ip$, $f$, and $d+id$ symmetries, whose form factors are illustrated in Fig. 3(c), Fig. 4(b), and Fig. 5(b), respectively. These different pairing symmetries can be distinguished by their different phase shifts upon each 60° rotation, which are $\pi/3$, $2\pi/3$, and $\pi$, respectively. The NNN-bond $p+ip$ and $f$-wave triplet pairings shown possess the following form factors:

$$f_{p+ip}(\delta_l) = e^{i(l-1)\frac{\pi}{3}}, \quad f_f(\delta_l) = (-1)^l, \quad l = 1,\ldots,6, \quad (6)$$

and the NN-bond singlet $d+id$ pairing shown possesses the form factor

$$f_{d+id}(\delta_l) = e^{i(l-1)\frac{2\pi}{3}}, \quad l = 1,2,3. \quad (7)$$

Note that the NN-bond pairing is prohibited in the $f$ symmetry. As for the $p+ip$ and $d+id$ pairings, although pairings on both the NN-bond and the NNN-bond are allowed, our DQMC calculations show that they are weaker (stronger) on the former than on the latter for the $p+ip$ ($d+id$) symmetry, reflecting the fact that the spin fluctuations on the former are less ferromagnetic like than those on the latter, consistent with our RPA calculations. We also studied longer-range pairings by adding third- and forth-bond pairings in the former factors, which turn out be much weaker than that of the NN-bond and NNN-bond presented above.

Our DQMC simulations of the system were performed at finite temperatures on a $2\times 48$, a $2\times 75$, and a $2\times 108$ lattices with periodic boundary conditions. Here, each lattice we employed in simulations consists of two interpenetrating triangular sublattices with hexagonal shape such that it

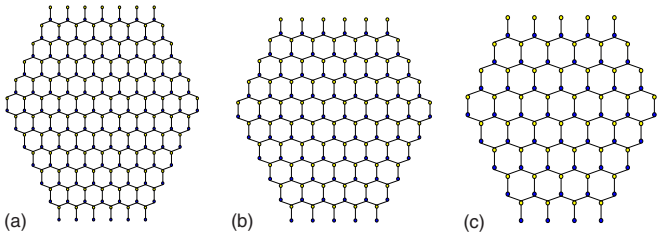


FIG. 6. (Color online) The lattice geometries for the (a) $2 \times 108$, (b) $2 \times 75$, and (c) $2 \times 48$ honeycomb lattices.

preserves most geometric symmetries of graphene, as shown in Fig. 6. In each case, the total number of unit cells is $3L^2$ and the total number of lattice sites is $2 \times 3L^2$ with $L = 6$, 5, or 4 in Figs. 6(a), 6(b), and 6(c), respectively. Figure 7 shows the temperature dependence of the pairing susceptibilities for different pairing symmetries with electron filling $n = 0.2$ [Fig. 7(a)] and $n = 0.1$ [Fig. 7(b)] with $U = 3t$. Within the parameter range investigated, the pairing susceptibilities for various symmetries increase as the temperature is lowered and, most remarkably, the $p + ip$ pairing symmetry dominates other symmetries at relatively low temperatures, consistent with the RPA results. In Fig. 7(a), the pairing susceptibility $P_{p+ip}$ on $2 \times 48$ and $2 \times 108$ lattices are also shown, in comparison with that on a $2 \times 75$ lattice, from which one verifies negligible finite-size effects.

The superconducting transition occurs as the pairing susceptibility diverges. However, DQMC simulations encounter the notorious minus problem in this doped system as well; consequently, the lower the temperature used in DQMC, the larger the error bar is. In Fig. 8, we simulated the system to the lowest temperature at our best while keeping a reasonable error bar. The lowest temperature for the $2 \times 75$ lattice is $t/12$ and the lowest temperature for the $2 \times 12$ lattice is $t/15$. Within our numerical results, we fit the DQMC data with a formula of $P = a/(T - T_c) + b$, as shown (dashed lines) in Fig. 8, and then we extrapolate to obtain $T_c$. The fit agrees with the DQMC data reasonably well. From this fit, one may estimate a $T_c$ of about $\sim 0.01t$, which is roughly $\sim 200$ K.

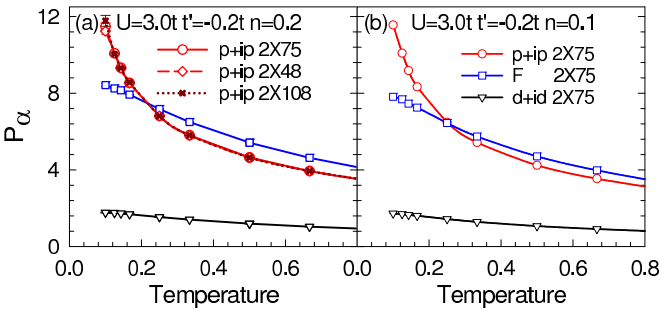


FIG. 7. (Color online) Pairing susceptibility $P_\alpha$ as a function of temperature for different pairing symmetries with $U = 3t$ at (a) $n = 0.2$ and (b) $n = 0.1$ on a $2 \times 75$ lattice (solid line). The $P_{p+ip}$ at $n = 0.2$ on a $2 \times 48$ lattice (dashed red line) and a $2 \times 108$ lattice are also shown (dotted red line) in panel (a). Here the units of temperature are $t$.

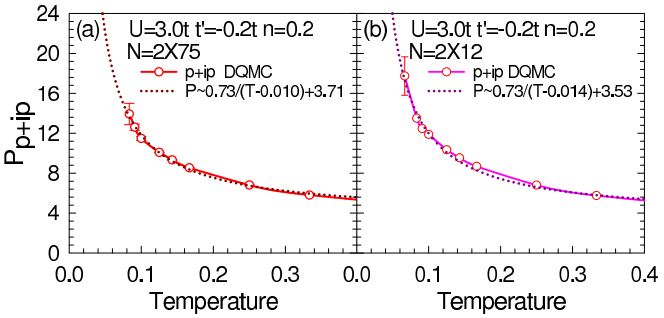


FIG. 8. (Color online) Pairing susceptibility $P_{p+ip}$ as a function of temperature with $U = 3t$ and $n = 0.2$ for (a) a $2 \times 75$ lattice and (b) a $2 \times 12$ lattice (solid line). The fits are shown as dashed lines.

In order to extract the intrinsic pairing interaction in our finite system, one should subtract from $P_\alpha$ its uncorrelated single-particle contribution $\widetilde{P}_\alpha$, which is achieved by replacing $\langle c^\dagger_{i\downarrow} c_{j\downarrow} c^\dagger_{i+\delta_l\uparrow} c_{j+\delta_{l'}\uparrow}\rangle$ in Eq. (4) with $\langle c^\dagger_{i\downarrow} c_{j\downarrow}\rangle\langle c^\dagger_{i+\delta_l\uparrow} c_{j+\delta_{l'}\uparrow}\rangle$. Clearly, in Fig. 9, the intrinsic pairing interaction $P_{p+ip} - \widetilde{P}_{p+ip}$ shows qualitatively the same temperature dependence as that of $P_{p+ip}$, which is positive and increases with decreasing temperature. Such a temperature dependence of $P_\alpha - \widetilde{P}_\alpha$ suggests effective attractions generated between electrons and an instability toward SC in the system at low temperatures. Moreover, Fig. 9(a) shows that the intrinsic pairing interaction for $p + ip$ symmetry enhances with larger $U$, indicating the enhanced pairing strength with the enhancement of the electron correlations. As for the other two pairing symmetries shown, our DQMC results yield negative intrinsic pairing interactions, reflecting the fact that the realization of the $p + ip$ symmetry at low temperatures will suppress other competing pairing channels.

## V. CONCLUSIONS AND DISCUSSIONS

We combined RPA analysis and DQMC calculations for the low-filled honeycomb Hubbard model with weak and strong repulsive $U$, respectively. Both studies show that triplet $p + ip$ SC occurs as the ground state of our model system of low-filled graphene. Besides graphene, the results obtained here also apply to other isostructure materials, such as silicene [31] and germanene [32]. Furthermore, by trapping some fermionic cold atoms into an optical lattice, one may also be able to simulate the Hubbard model on the honeycomb lattice studied

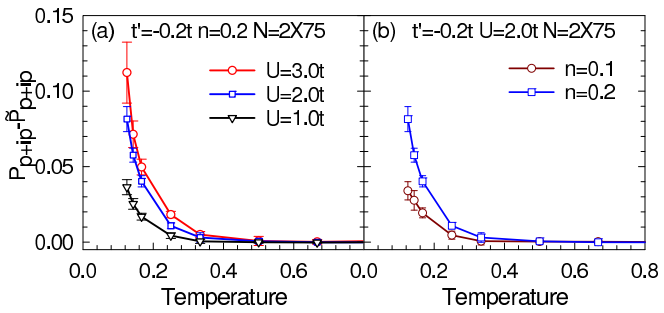


FIG. 9. (Color online) The intrinsic pairing interaction $P_{p+ip} - \widetilde{P}_{p+ip}$ as a function of temperature for (a) different $U$ and (b) different $n$ on a $2 \times 75$ lattice.

here [33–35], with tunable parameters and dopings, which is expected to realize triplet $p+ip$ superfluidity.

## ACKNOWLEDGMENTS

We would like to thank Zhong-Bin Huang, Yuigui Yao, Yu-Zhong Zhang, and Su-Peng Kou for stimulating discussions. This work is supported in part by NSFC Grants No. 11104014, No. 11274041, No. 11374034, and No. 11334012, by the Research Fund for the Doctoral Program of Higher Education of China 20110003120007 and SRF for ROCS (SEM) (T.M.), by the NCET program under Grant No. NCET-12-0038 (F.Y.), and the Thousand-Young-Talent Program of China and the NSFC under Grant No. 11474175 (H.Y.).

[1] K. S. Novoselov, A. K. Geim, S. V. Morozov, D. Jiang, Y. Zhang, S. V. Dubonos, I. V. Gregorieva, and A. A. Firsov, Science **306**, 666 (2004).
[2] For a review, see A. H. Castro Neto, F. Guinea, N. M. R. Peres, K. S. Novoselov, and A. K. Geim, Rev. Mod. Phys. **81**, 109 (2009).
[3] S. Raghu, S. A. Kivelson, and D. J. Scalapino, Phys. Rev. B **81**, 224505 (2010).
[4] R. Nandkishore, R. Thomale, and A. V. Chubukov, Phys. Rev. B **89**, 144501 (2014).
[5] R. Nandkishore, L. S. Levitov, and A. V. Chubukov, Nat. Phys. **8**, 158 (2012).
[6] W.-S. Wang, Y.-Y. Xiang, Q.-H. Wang, F. Wang, F. Yang, and D.-H. Lee, Phys. Rev. B **85**, 035414 (2012).
[7] M. L. Kiesel, C. Platt, W. Hanke, D. A. Abanin, and R. Thomale, Phys. Rev. B **86**, 020507(R) (2012).
[8] A. M. Black-Schaffer and S. Doniach, Phys. Rev. B **75**, 134512 (2007).
[9] J. González, Phys. Rev. B **78**, 205431 (2008).
[10] S. Pathak, V. B. Shenoy, and G. Baskaran, Phys. Rev. B **81**, 085431 (2010).
[11] C. Platt, W. Hanke, and R. Thomale, Adv. Phys. **62**, 453 (2013).
[12] X.-L. Qi and S.-C. Zhang, Rev. Mod. Phys. **83**, 1057 (2011).
[13] M. Z. Hasan and C. L. Kane, Rev. Mod. Phys. **82**, 3045 (2010).
[14] T. Li, Europhys. Lett. **97**, 37001 (2012).
[15] I. Martin and C. D. Batista, Phys. Rev. Lett. **101**, 156402 (2008).
[16] H. Yao and F. Yang, arXiv:1312.0077.
[17] X. Chen, Y. Yao, H. Yao, F. Yang, and J. Ni, arXiv:1404.3346.
[18] J. Jung and A. H. MacDonald, Phys. Rev. B **87**, 195450 (2013).
[19] A. Kretinin, G. L. Yu, R. Jalil, Y. Cao, F. Withers, A. Mishchenko, M. I. Katsnelson, K. S. Novoselov, A. K. Geim, and F. Guinea, Phys. Rev. B **88**, 165427 (2013).
[20] R. S. Deacon, K. C. Chuang, R. J. Nicholas, K. S. Novoselov, and A. K. Geim, Phys. Rev. B **76**, 081406 (2007).
[21] J. T. Ye, S. Inoue, K. Kobayashi, Y. Kasahara, H. T. Yuan, H. Shimotani, and Y. Y. Iwasa, Nat. Mater. **9**, 125 (2010).
[22] T. Ma, F. M. Hu, Z. B. Huang, and H. Q. Lin, Appl. Phys. Lett. **97**, 112504 (2010).
[23] N. E. Bickers, D. J. Scalapino, and S. R. White, Phys. Rev. Lett. **62**, 961 (1989).
[24] D. J. Scalapino, Rev. Mod. Phys. **84**, 1383 (2012).
[25] T. Takimoto, T. Hotta, and K. Ueda, Phys. Rev. B **69**, 104504 (2004); K. Yada and H. Kontani, J. Phys. Soc. Jpn. **74**, 2161 (2005).
[26] K. Kubo, Phys. Rev. B **75**, 224509 (2007); K. Kuroki, S. Onari, R. Arita, H. Usui, Y. Tanaka, H. Kontani, and H. Aoki, Phys. Rev. Lett. **101**, 087004 (2008).
[27] S. Graser, T. A. Maier, P. J. Hirschfeld, and D. J. Scalapino, New J. Phys. **11**, 025016 (2009).
[28] F. Liu, C.-C. Liu, K. Wu, F. Yang, and Y. Yao, Phys. Rev. Lett. **111**, 066804 (2013); L.-D. Zhang, F. Yang, and Y. Yao, arXiv:1309.7347.
[29] R. Blankenbecler, D. J. Scalapino, and R. L. Sugar, Phys. Rev. D **24**, 2278 (1981).
[30] T. Ma, F. M. Hu, Z. B. Huang, and H.-Q. Lin, *Horizons in World Physics* (Nova Science, Hauppauge, New York, 2011), Vol. 276, Chap. 8.
[31] B. Lalmi, H. Oughaddou, H. Enriquez, A. Karae, S. Vizzini, B. Ealet, and B. Aufray, Appl. Phys. Lett. **97**, 223109 (2010).
[32] M. E. Dvila, L. Xian, S. Cahangirov, A. Rubio, and G. Le Lay, arXiv:1406.2488.
[33] S.-L. Zhu, B. G. Wang, and L.-M. Duan, Phys. Rev. Lett. **98**, 260402 (2007).
[34] C. J. Wu, D. Bergman, L. Balents, and S. Das Sarma, Phys. Rev. Lett. **99**, 070401 (2007).
[35] L. Tarruell, D. Greif, T. Uehlinger, G. Jotzu, and T. Esslinger, Nature (London) **483**, 302 (2012).